OGO-2 MAGNETIC FIELD OBSERVATIONS DURING THE MAGNETIC STORM OF MARCH 13-15, 1966

By

R. A. Langel
and
J. C. Cain

October 1967

(Presented at the IAGA Special Events Symposium, St. Gall, Switzerland, October 2, 1967. The symposium proceedings are planned for publication in the Annales de Geophysique).

Abstract

Magnetic field data from the OGO-2 spacecraft and from surface magnetic observatories are analyzed for the period March 13-15, 1966. During this interval there occurred a magnetic storm with a Dst decrease of 122γ.

The results indicate a non-symmetric inflation of the magnetosphere (asymmetric ring current) with the field decrease in the dusk sector a factor of about three more than that in the dawn sector. Within the 10-30γ accuracy of the data, the field disturbance at the satellite was equal to that on the surface at the same local time. From this evidence it is concluded that the source of both Dst and DS in low latitudes are external to the satellite altitudes (410-1510 km). The disturbance observed near the dusk meridian commenced several hours sooner than that observed near the dawn meridian, reached its maximum intensity in 18 hours and then decayed in another 18 hours to the level seen on the dawn meridian.

Polar ionospheric currents were detected more than 1.5 hours before the storm's main phase. These currents conform to the classical "two celled" model which includes a concentrated eastward current in the evening local time sector and a concentrated westward current in the morning local time sector. The evening currents first appear at L=7.5 and smoothly shift to L=4.3 at the time of maximum Dst. The morning currents first appears at L=7.9 and subsequently shift to L=5.3. The L location of the morning currents is always greater than that of the evening currents. These currents decrease at least by an order of magnitude at the same time as the transition from asymmetric to symmetric inflation is seen at low latitude.

RESUMÉ

Les résultats de champ magnétique observés du vehicule spatiale OGO-2 et des observatoires magnétiques de surface sont analysés du 13 au 15 Mai 1966. Pendant cette période un orage magnétique eût lieu avec une réduction Dst de 122 γ.

Les résultats indiquent une inflation non-symétrique de la magnétosphère (courant circulaire asymétrique) dont le champ decroît dans le secteur crépusculaire d'un facteur environ 3 fois supérieur à ce dont il decroît à l'aube. Considerant le degré d'erreur de 10 à 30 γ, le champ de perturbation mesuré au satellite fut égal à celui pris à la surface au même temps local. De cette observation, l'on conclut que la source des deux Dst et Ds en basses latitudes sont en dehors des altitudes (410 - 1510 km) du satellite. La perturbation observée près du meridien crépusculaire a commencé quelques heures plus tôt que celle observée près du meridien de l'aube, elle atteint son intensité maximum en 18 h, et puis decroît en 18 h encore jusqu'au niveau vu dans le meridien de l'aube.

Des courants polaires dans la ionosphère ont été detectés plus de 1 h 1/2 avant la phase principale de l'orage. Ces courants se conforment au modèle classique "a deux cellules", qui correspond à un courant concentré vers l'Est dans l'espace de temps correspondant au soir du temps local, et d'un courant concentré vers l'Ouest dans l'espace de temps correspondant au matin du temps local. Les courants du soir apparaissent d'abord à L = 7,5 et se déplacent doucement vers L = 4,3 au temps de Dst maximum. Les courants du matin apparaissent d'abord à L = 7,9 et ensuite se déplacent vers L = 5,3. La position L des courants du matin est toujours supérieure à celle des courants du soir. Ces courants decroissent d'au moins un facteur 10 en même temps que la transition d'asymétrique à symétrique inflation est vue en basses latitudes.

Introduction

The magnetic storm in mid-March 1966 is the first large disturbance encountered by the OGO-2 spacecraft* (launched October 14, 1965) and one of the earliest significant events following the sunspot minimum years 1964-65. It provides magnetic field variations of a sufficiently large amplitude that it is possible to make a synoptic analysis of the magnetic variations recorded by OGO-2 without resorting to sophisticated computations to eliminate such effects as the solar quiet daily variation (Sq) and to be overly concerned about baseline errors caused by orbital and reference field uncertainties.

This storm thus gives the first opportunity to investigate such questions as whether the storm-time disturbance seen at the surface are due partly or wholly to ionospheric currents as has been speculated in the past. As first noted by Heppner, Stolarik, and Meredith (1958), the satellite magnetic observations will definitively sort out the extent to which the source is below or above its altitude.

The ambient magnetic field near the earth consists of the main internal field together with its secular change and crustal anomalies, and of shorter period time varying changes. Among these short period changes is the disturbance variation (D) resulting from geomagnetic storms. D has been exhaustively analyzed from surface data (e.g. Chapman, 1919, 1927, 1935, 1952; Sugiura and Chapman, 1960) and until recently has been partitioned into only the two components Dst and DS. Dst is defined as the part of D symmetrical with the earth's dipole

---

*Sometimes also referred to by its prelaunch designation OGO-C, POGO-1 (Polar Orbiting Geophysical Observatory-1) and its satellite number 1965-81A.

axis (i.e. the average of D around a dipole latitude) and DS as the residual D minus Dst.

Dst and DS are usually represented in terms of equivalent ionospheric current systems (see, for example, Vestine et al., 1949) although Dst is thought to result from an extra terrestrial ring current located in the radiation belts. DS has generally been considered to result from return currents of an intense polar current, the polar electrojet, associated with precipitation of particles and with auroral phenomena.

The results of the Vanguard 3 satellite magnetic field measurements clearly showed that the average changes of Dst in the 500-2400 Km range paralleled those at the surface near the equator and hence were from a source external to the satellite (Cain et al., 1962). However, the data were too sparse to draw any conclusions about whether the asymmetric component DS is below or above the satellite altitude.

The polar patterns of the disturbance field is less simple than that observed at lower latitudes and has been differently interpreted by different workers.

Two conflicting models of polar current systems are illustrated in Figure 1. The earlier model, A in the figure, was initially developed by Chapman (e.g. 1935) and later refined (e.g. by Vestine, 1949). This model has two current cells. One cell has an intense westward electrojet, centered between about 0200 - 0500 hours local time, with eastward return currents to the north and south. The other cell has an intense eastward electrojet between about 1600 - 2200 hours local time with westward return currents to the north and south.

Recently, a new one-celled polar electrojet model (B in Figure 1) has been proposed by Akasofu et al. (1965) in which the primary electrojet is always westward in direction. In the evening sector they indicate an intense westward current in more northern latitudes where earlier researchers would have placed a westward return current from a more southerly eastward electrojet. In a study of the records of magnetic sub-storms at Lerwick and two close by temporary stations, Scrase (1967) has also deduced this one-celled type of current system.

The purpose of this paper is to examine and correlate surface and satellite magnetic field measurements so as to examine the major features of the disturbance field during the storm of March 13-15, 1966. We will show that the low and middle latitude asymmetric portion of the disturbance feature (DS) is not primarily ionospheric in origin and will discuss the differences in the low latitude disturbance field at local dawn and dusk. We will also discuss the location and intensity of the polar electrojet, showing its relation to dip latitude, geomagnetic latitude, and McIlwain's L parameter, and will demonstrate that the data from this storm supports the two-celled electrojet model rather than the one-celled model.

The OGO-2 Magnetic Field Experiment

OGO-2 was launched on 14 October 1965 into an orbit with the following characteristics:

inclination	87.4°
perigee	413 km
apogee	1510 km
anomalistic period	104.3 min.

For a summary of the experiment operation and of the data processing techniques used to reduce the data see Cain et al. (1967) and Langel (1967). During March 13-14, 1966, the OGO-2 orbital plane was in the twilight meridian with ascending node at about 0440 hours local time and descending node at about 1630 hours local time; perigee was near 72°N on the ascending (dawn) side of the orbit.

The magnetic field experiment on OGO-2 measured the total (scalar) field with an accuracy better than $\pm 2\gamma$ (gammas) and a resolution of $\pm .43\gamma$ (Farthing and Folz, 1967). Data were taken at half-second intervals. Figure 2 is a typical plot of one orbit of OGO-2 data on a geomagnetically quiet day (October 19, 1965). Vertical grid lines are labeled according to latitude while the time (UT, hours and minutes) longitude and altitude are given at the short vertical tic marks. The bottom plot is the measured data and the top plot is measured data minus a theoretical field (ΔF) computed using the GSFC(12/66) spherical harmonic expansion (Cain et al., July 1967). Both scales are in gammas.

The ambient field measured at OGO-2 altitudes contains possible contributions from all of the sources discussed in the introduction.

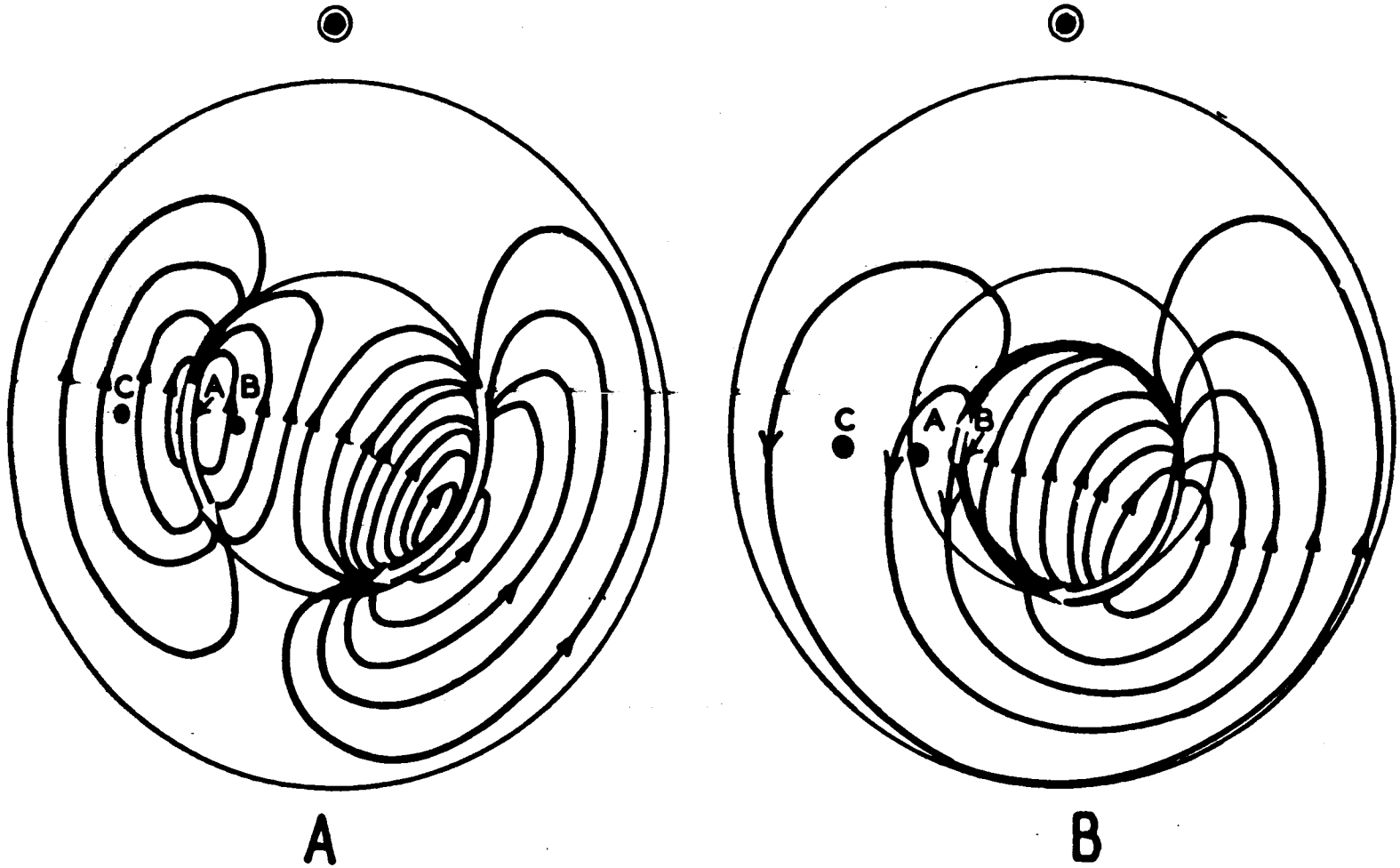

Earlier model current system (schematic) for polar magnetic substorm; view from above dp. north pole; the direction of the sun is indicated.

Proposed model current system (schematic) for polar magnetic substorm; view from above dp. north pole; the direction of the sun is indicated.

FIG 1. POLAR CURRENT MODELS (AKASOFU, ET. AL., 1965)

FIGURE 1

The GSFC(12/66) reference model used to eliminate the effect of the main field from the data contains 120 spherical harmonic coefficients of the internal potential. A simple subtraction of this reference from the measured field gives the quantity $\Delta F = |\bar{M} + \bar{D} + \bar{Q}| - |\bar{M}|$ where $\bar{Q}$ is the quiet day contribution present on all days and $\bar{D}$ the vector due to magnetic disturbance. The effect of any crustal anomalies is assumed to be either negligible or included in $\bar{M}$. Since a sample of OGO-2 data taken during a quiet interval in November, 1965 was included in the derivation of the GSFC(12/66) field model, it is likely that this model provides a good reference at near quiet conditions. As pointed out in the evaluations for this model (Cain et al., 1967) the errors are likely to be in the 10-30γ range from OGO-2 altitudes for epochs 1965-1970. This is borne out by the ΔF portion of Figure 2 where the maximum difference between measured and computed field is about 30γ. This plot is very typical of all the non-storm data examined to this date, particularly in the equatorial regions. Larger departures sometimes occur in polar regions which are probably due to a ionospheric current near the auroral zone. These errors are of the same order of magnitude as the quiet daily variation. Thus, if one confines the considerations of OGO-2 data to a region where $\bar{D}$ and $\bar{M}$ are roughly parallel, as at low latitudes, and for storms where $D \gg Q$, then ΔF becomes a good approximation to D.

Since the vector magnetic field is predominantly horizontal at low latitudes, the change in total magnetic force (ΔF) will be very nearly equal to the horizontal (H) disturbance. OGO-2 measures ΔF

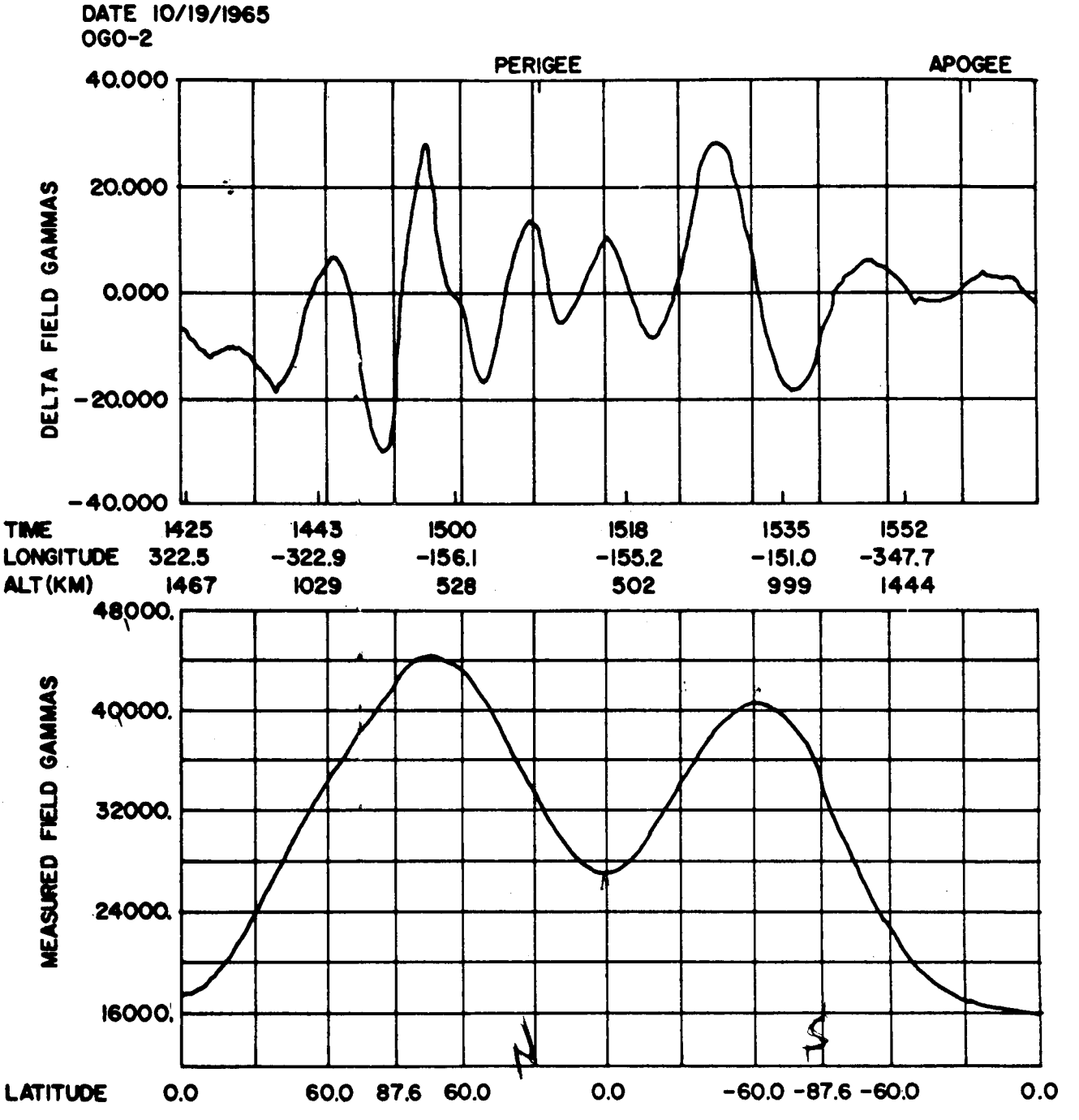

Typical Quiet Day Plot Of Satellite Data

FIGURE 2

above the ionosphere and therefore ionospheric currents causing an H disturbance on the surface of earth would cause a disturbance in the opposite direction at the satellite (Heppner et al, 1958).

PART I - THE ASYMMETRIC RING CURRENT

Surface Observations

Figure 3 is a plot of (provisional) Dst (Hendricks, 1967) for March 13-15, 1966. Thus was computed using techniques described by Sugiura (1964) and Sugiura and Hendricks (1967). The observatories utilized were Honolulu, Hermanus, and San Juan. The plot gives this provisional Dst in gammas as a function of Universal Time for 72 hours commencing at zero hours UT on March 13. Arrows indicate approximate times of occurrence of (descending node) equatorial crossings of the OGO-2 data shown in Figure 8.

The main phase of this moderate storm commences gradually at about 1900 UT on March 13th, with the largest disturbance occurring at about 0500 UT on the 14th. Recovery takes place in two phases; there is a fairly rapid recovery to a level of -30γ between 0500 UT and 1100 UT on the 14th, and a slower recovery continuing into March 16 and 17.

The asymmetric aspects of this storm are also typical. Figure 4 (Sugiura and Chapman, 1960) shows average SD variations as a function of both latitude and storm intensity. The curves are computed separately for each of the first three storm days. For mid-low latitudes the curves all have the same general characteristics. The maximum positive disturbance is always in local morning and the maximum negative disturbance in local evening. If we consider all of the DS disturbance to be in a negative (decreasing H) direction, then the minimum disturbance

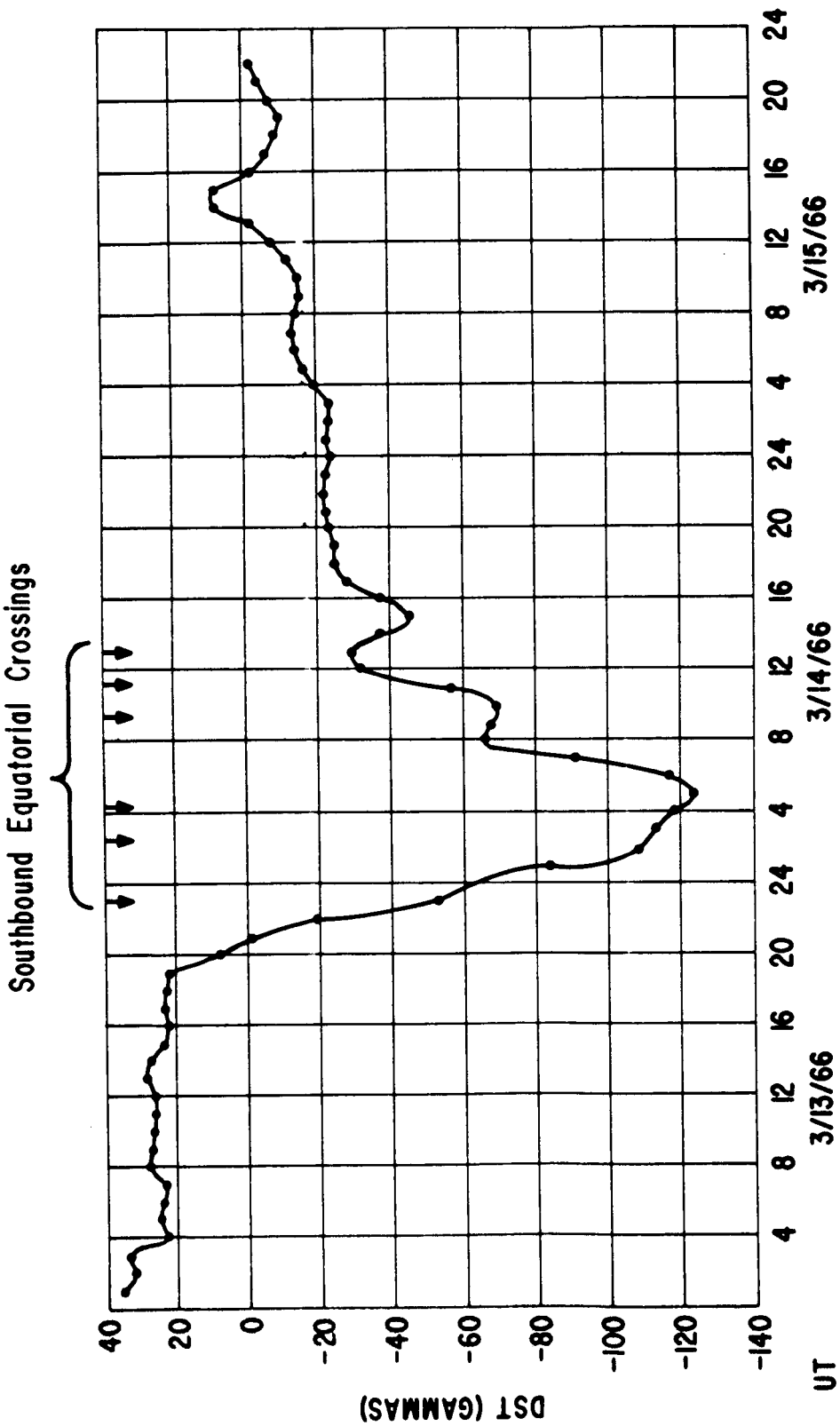

Dst For March 13-15, 1966

FIGURE 3

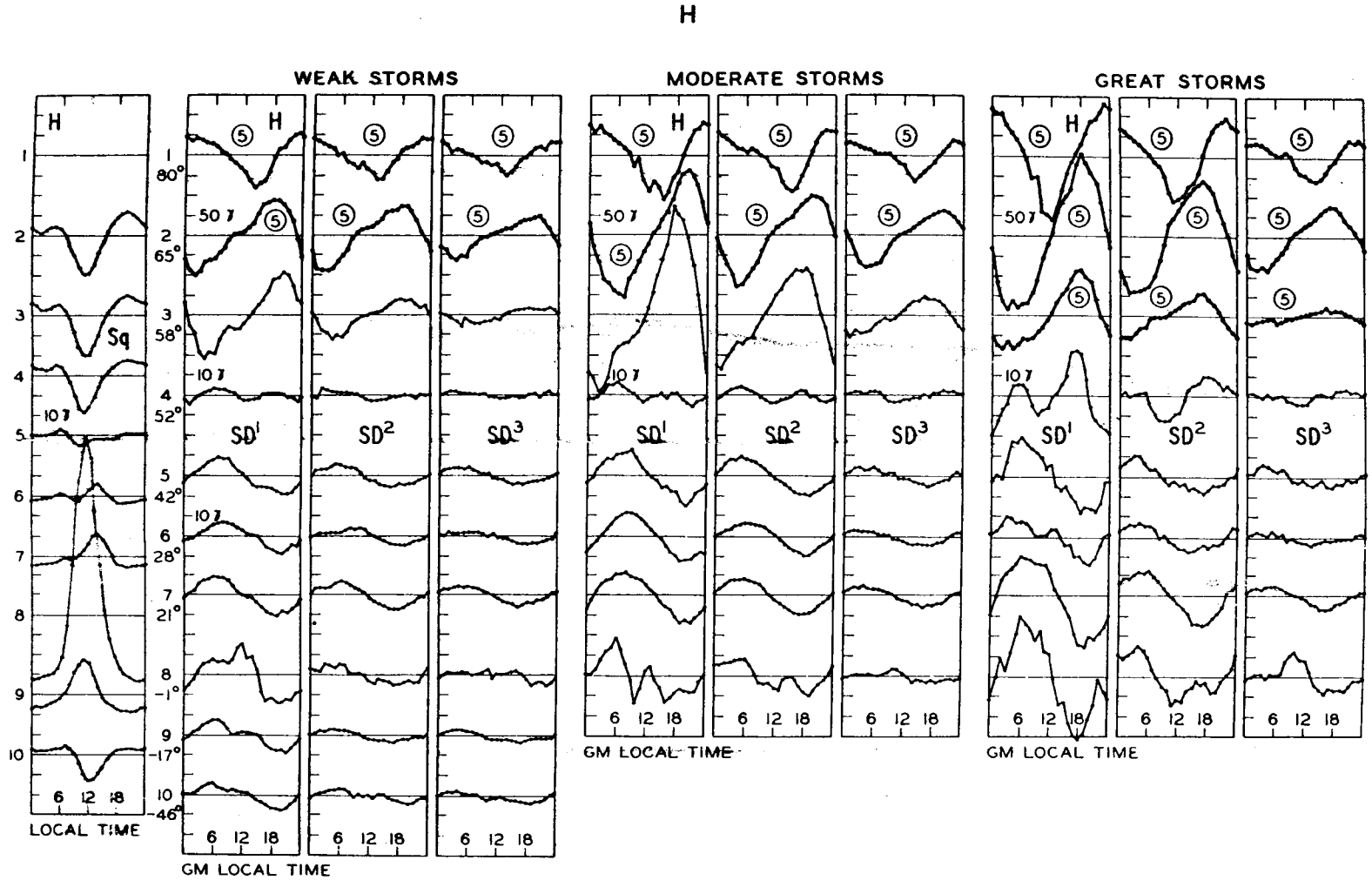

Sq and SD in the horizontal force H (*not* the geomagnetic north component Hgm). The first panel illustrates Sq; the following three sets (of three panels each) refer to the three intensity sets, in the order weak, moderate and great: each set gives SD^n (n = 1, 2, 3) for the first three storm days. The force scale is uniform except where otherwise indicated by a number (the scale contraction factor) enclosed in a circle. The abscissae for Sq refer to standard local time; those for SD refer to gm local time.

Examples of SD During Magnetic Storms (Sugiura and Chapman, 1960)

FIGURE 4

due to DS occurs at local morning and the maximum disturbance at local evening.

Figure 5 is a set of 15 magnetograms (horizontal component) from low and mid-latitude observatories for the March 1966 storm, with station abbreviation and dip latitude given along the ordinate. The plot begins at zero hours UT on March 13 and extends to zero hours on the 15th. Each division on the ordinate is 100γ. The magnetograms are arranged according to station longitude and an arrow indicates 0600 hours local time on each plot. Each plot exhibits a smaller negative disturbance vector in the early morning hours of local time (this feature is darkened on each plot for emphasis). The extent and detailed characteristics of this feature vary from station to station but it is present at each station at approximately the same local time and with approximately the same magnitude. Figure 5 indicates that the major part of this asymmetrical feature is in the early morning hours during the start of the storm. At about 6 hours UT, March 15, (the M'Bour magnetogram) a broadening commences which continues as the storm goes into the recovery phase.

Some researchers have suspected that the main features of DS might not be ionospheric. Akasofu and Chapman(1964) analyzed several magnetic storms in which they found a definite asymmetry in the H disturbance vector in mid and low latitudes. Figure 6, from their paper, shows the distribution of the H disturbance at two hour intervals during a storm. The disturbance fields depicted are local

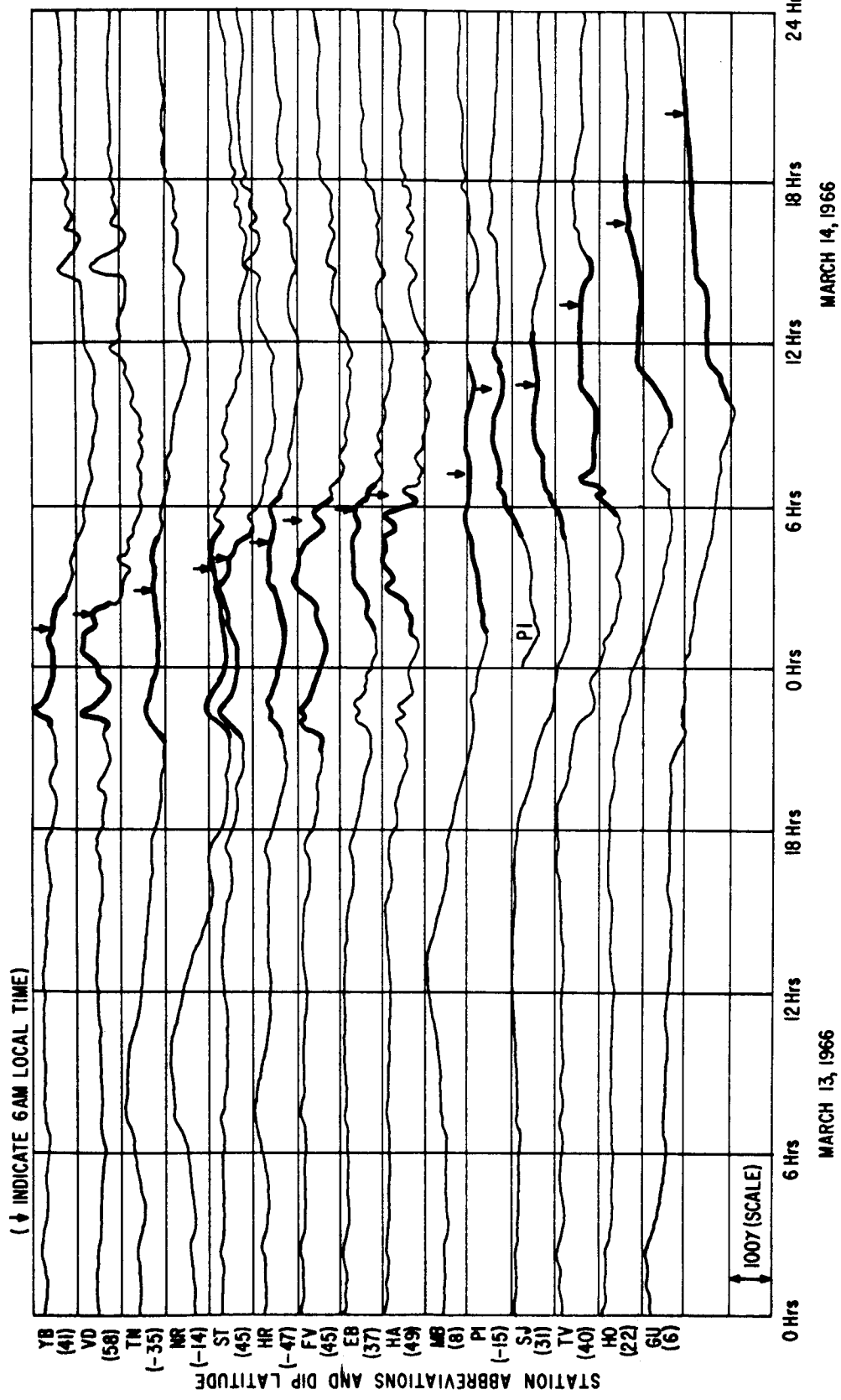

Low and Mid Latitude Magnetograms Arranged By Local Time, Horizontal Component

Stations included are Yangi-Bazar, Vysokaya Dubrava, Tananarive, Nairobi, Stepanovka, Hermanus, Furstenfeldbruck, Ebro, Hartland, M'Bour, Pilar, San Juan, Tucson, Honolulu, and Guam.

FIGURE 5

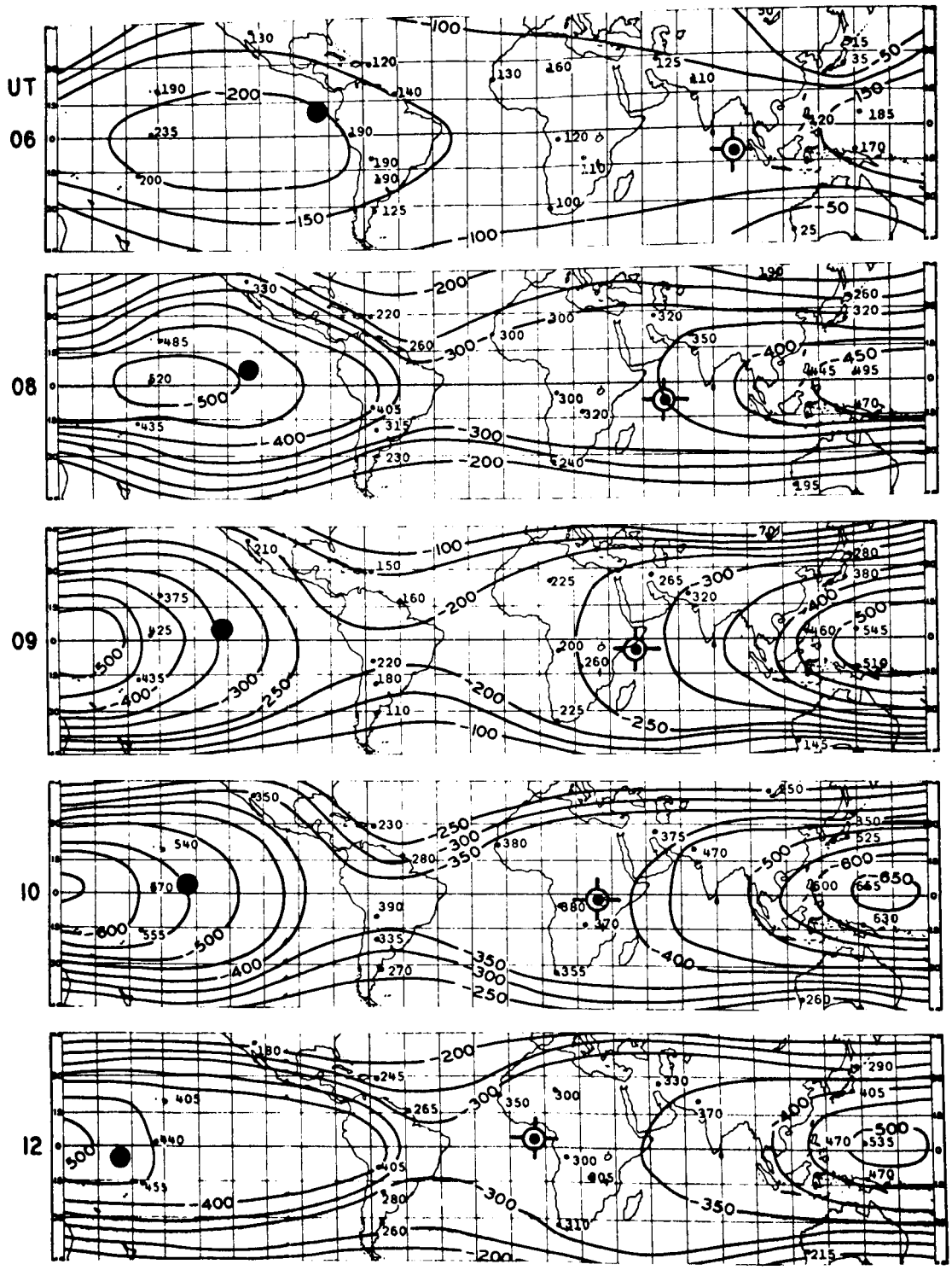

THE DISTRIBUTION OF THE HORIZONTAL COMPONENT OF THE DISTURBANCE FIELD, $D(H)$, AT 0600, 0800, 0900, 1000 AND 1200 GMT, 13 SEPTEMBER 1957. THE SUBSOLAR POINT IS INDICATED BY A RAYED OPEN CIRCLE AND THE ANTI-SUBSOLAR POINT BY A BLACK CIRCLE.

FIGURE 6: Asymmetry in H Disturbance (Akasofu and Chapman, 1964)

time dependent, the greatest disturbance occurring during the local evening and least during local morning. They concluded from magnetogram evidence that the asymmetry did not result from return ionospheric currents of an auroral electrojet.

A similar plot (Figure 7) is shown for 3:00 UT on March 14, 1966. The stations available (indicated by * on the figure) were rather sparse and the contours are hand drawn. While the disturbance is not as large as those examined by Akasofu and Chapman, the asymmetry is very similar.

OGO-2 Storm Data

Figure 8 is a plot of several orbits of data from the OGO-2 satellite, the earlier orbits are at the bottom of the figure. The approximate times of these plots are indicated by arrows in Figure 3. As in the top of Figure 2, the quantity plotted is the measured field minus a theoretical field (ΔF) using the GSFC(12/66) spherical harmonic representation (Cain et al., 1967). The southbound equatorial crossings occur at about 1630 hours local time (local evening) and the northbound equatorial crossings occur at about 0440 hours local time (local morning). The numbers in parenthesis indicate extreme excursions on the plot. The amount of disturbance at local evening is always larger than that at local morning, usually more than twice as large. This asymmetry is in the same direction as that observed on the surface, indicating that the current source is above the satellite.

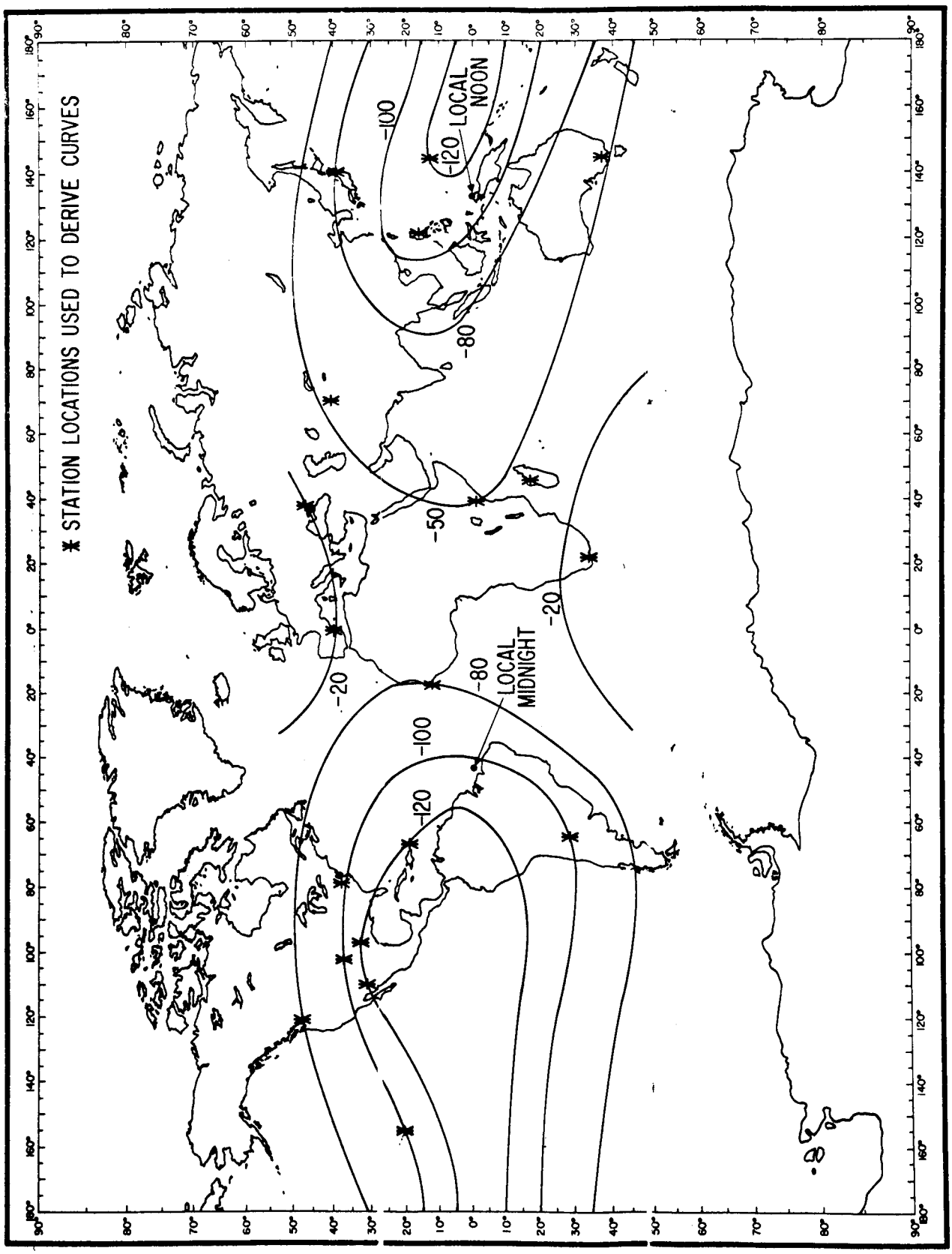

The Distribution of the Horizontal Disturbance Field
At 0300 UT on March 14, 1966. (Units are gammas.)

FIGURE 7

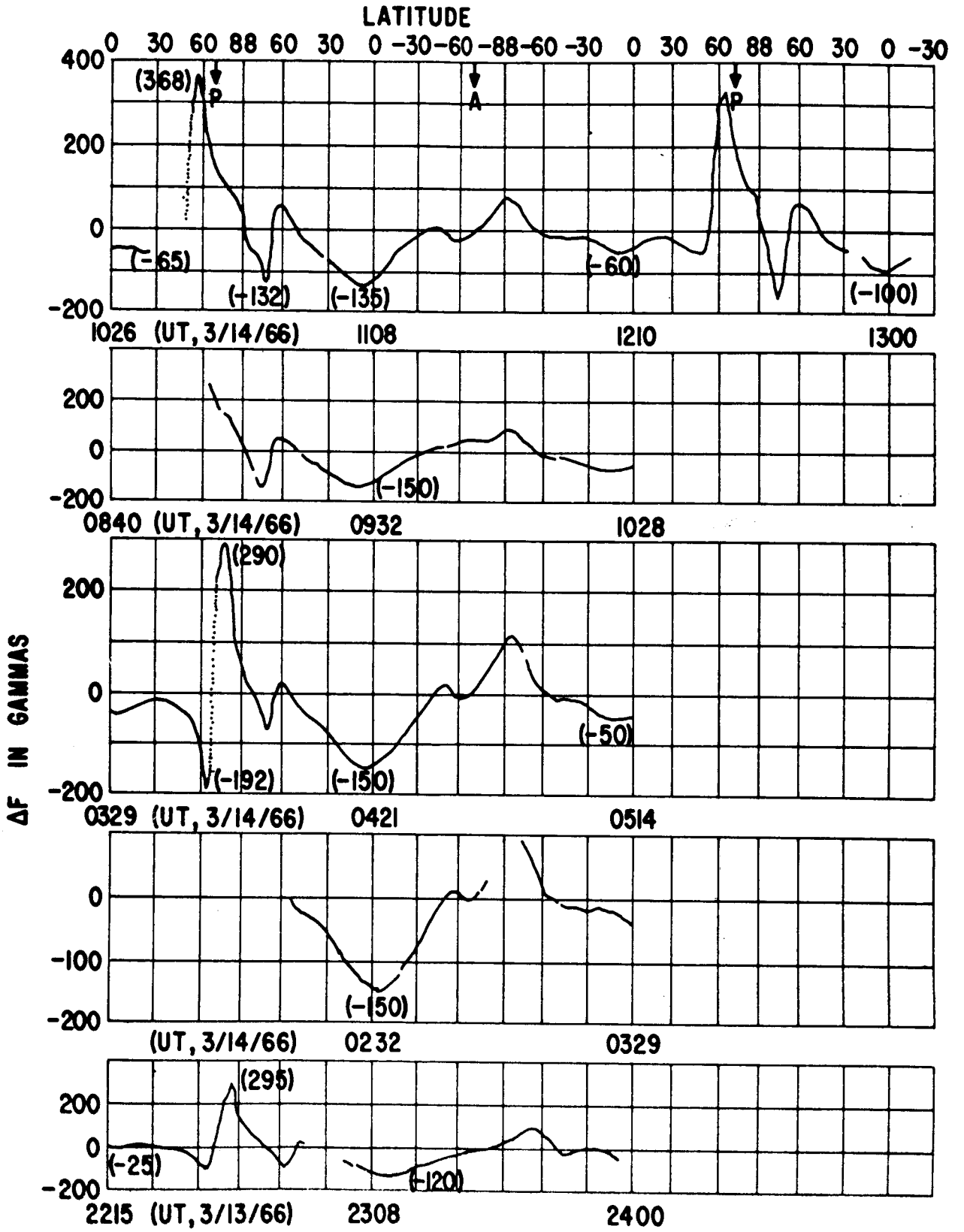

Measured Minus Computed Field From the OGO-2 Satellite During the March 13-15, 1966 Magnetic Storm

FIGURE 8

Surface-Satellite Comparisons

In order to better examine the spacecraft-surface correlation we drew the composite plots of Figure 9. The abscissa is time (UT) and the ordinates of the various plots are in gammas. The top curve is the previously mentioned provisional Dst. The next two curves are derived from satellite data. Each point was determined by finding the maximum deviation (ΔF) between $+30^{\circ}$ and -30° in latitude, on a single satellite pass. The morning and evening data are plotted separately; the dashed horizontal lines indicate the pre-storm level. The bottom two curves are derived from low latitude observatory data. The disturbance in H at 6 A.M. and 6 P.M. (local time) from low latitude observatories*, widely dispersed in longitude, is plotted as a function of UT (this does not vary significantly from that at 0440 and 1630, the satellite local times.) Again, the morning and evening data are plotted separately.

It is immediately clear that the disturbance at satellite altitudes is almost identical to that on the surface. The asymmetry in H disturbance in the satellite data correlates both in direction and magnitude with the surface data. The cause of at least the major portion of the asymmetry (or the DS) must therefore be sought in regions above the altitude of the satellite.

Another significant feature of Figure 9 is the way the evening curves taper off in the recovery phase of the storm. Both the satellite and observatory evening data seem to rise to a level which is

---

* Almeria, Bangui, Guam, Honolulu, M'Bour, San Juan, Tananarive, Tucson

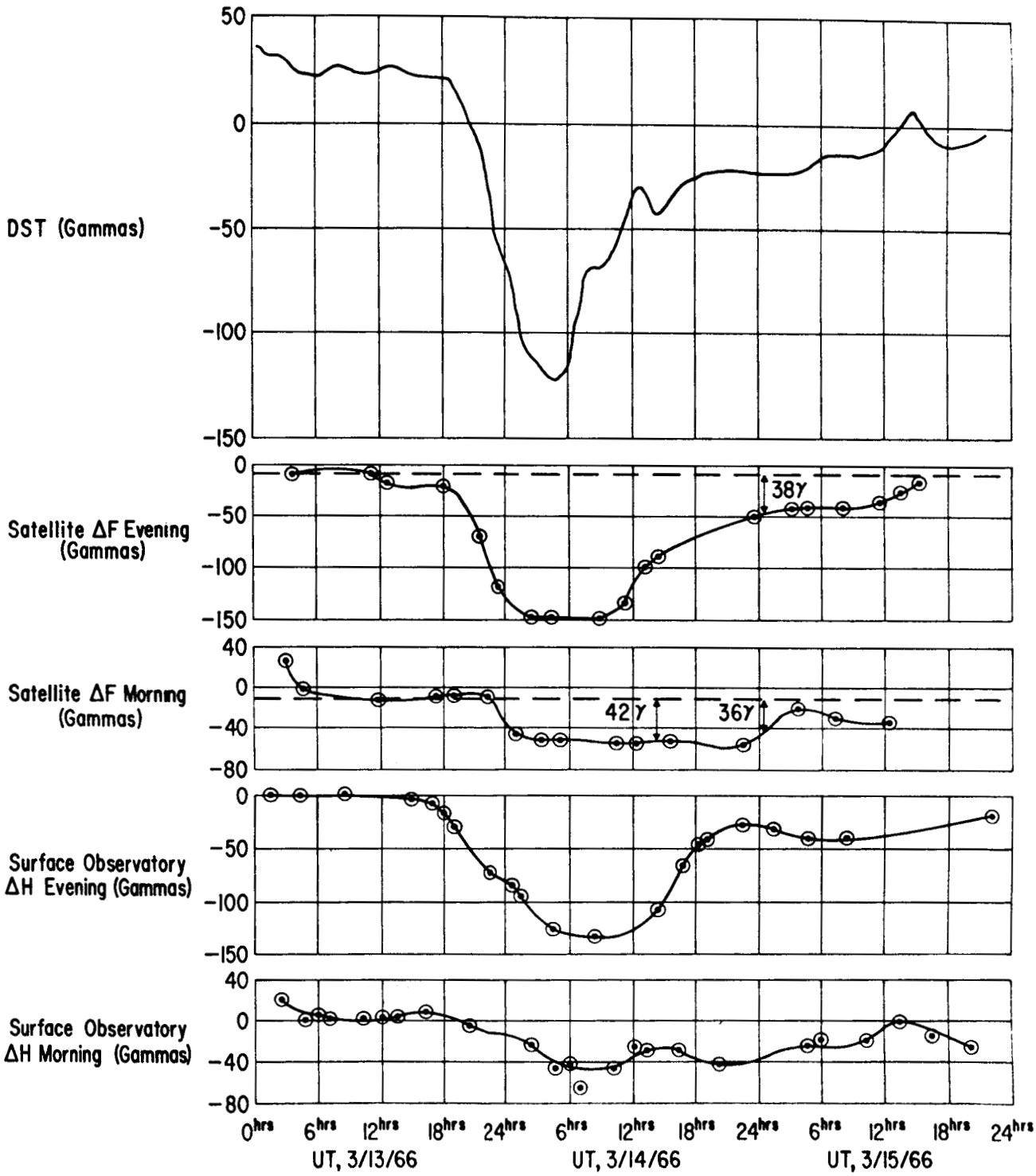

FIGURE 9: Comparison of Dst, Satellite and Surface Observatory Data. The satellite data are the points of maximum deviation between +30° and -30° latitude. The morning satellite data is 0440 local time and the evening is at 1630 local time. The observatory data are the 0600 and 1800 local time values of D(H) at seven low latitude observatories.

within a few gammas of the maximum disturbance in the morning hours. (cf. the satellite evening curve at 2400 hours on the 14th with the satellite morning curve at 1200 hours on the 14th.) Also, the morning data retain the maximum level of disturbance much longer than the evening data. Close examination of the satellite data also suggests the possibility that there is approximately a four hour delay in the start of the morning disturbance after the evening data has begun its downswing.

The relationship between the field depressions in the morning and evening sectors is more clearly presented by plotting the ΔF derived from the satellite data versus Universal Time, selecting only data points at zero degrees dip latitude. This is done in Figure 10. The abscissa is UT and the ordinate is ΔF in gammas. Morning and evening data are clearly distinguishable. The pre-storm depression is approximately the same for both local times. However, the evening data is well into its downswing by 2200 on the 13th while the morning data has not yet left its pre-storm value. Commencement of the morning depression occurs more suddenly than the evening and retains its maximum level of depression after the evening data has begun its fast recovery. From zero hours on the 15th onward the curves are for all intents indistinguishable except for one isolated point in the morning data.

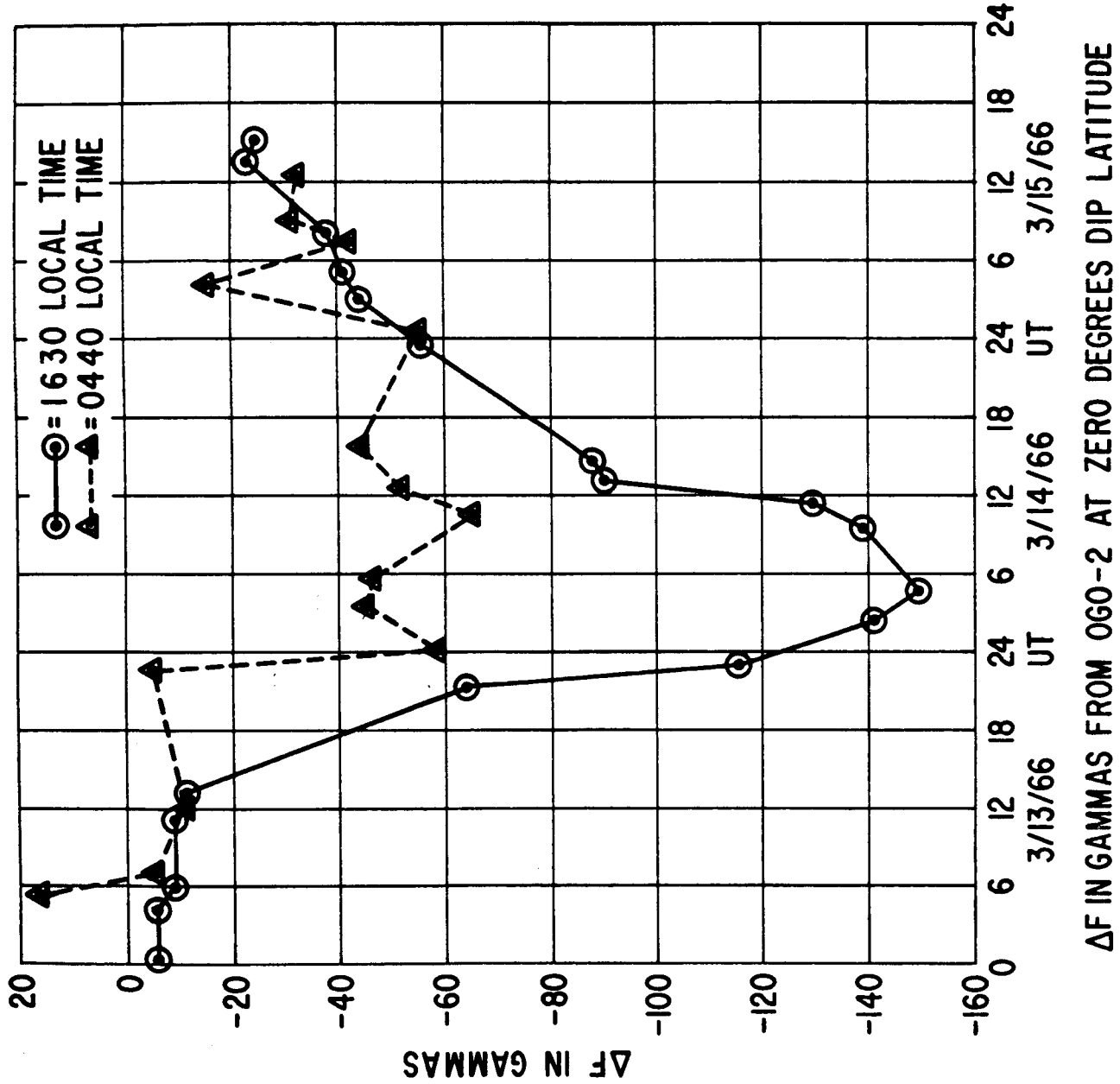
1630 LOCAL TIME
0440 LOCAL TIME
ΔF IN GAMMAS
20
0
-20
-40
-60
-80
-100
-120
-140
-160
0
6
12
18
24
3/13/66
UT
3/14/66
3/15/66
ΔF IN GAMMAS FROM OGO-2 AT ZERO DEGREES DIP LATITUDE

FIGURE 10

Discussion

Parker (1966) has discussed some theoretical properties of non-symmetric inflation of a magnetosphere. He points out that this non-symmetric inflation will result in rapid dissipation of the contributing particles so that the non-symmetry should be confined to the active phase of a magnetic storm. In support of this, Cahill (1966) reports that the magnetometer data from Explorer 26 (1.05 R_e to 5.11 R_e) indicated an asymmetric inflation, with a body of charged particles either introduced or locally accelerated in the evening local time quadrant (1800 to 2400 local time). He then observed a rapid shift to an axially symmetric ring current which then persisted for several days.

The OGO-2 data support this type of picture. It is clear that from 2200 UT on the 13th to 1200 UT on the 14th the disturbance both in the OGO-2 data and the surface data indicate a substantially larger inflation during evening local time than during the morning hours. At 2400 UT on the 14th the disturbances at both local times reach comparable levels and then remain comparable throughout the slow recovery phase. The time lag between the morning and evening hours may indicate injection of particles in the evening sector and then a spread of some of these particles symmetrically to form the entire ring current. Figure 10 would indicate a time lag of about six hours for the particles forming the symmetric belt to travel from 1630 local time to 0440 local time.

Thus, for the storm of March 13-14, 1966, the sources of both Dst and DS are external to the satellite data. This strongly supports theories of a non-symmetric inflation of the magnetosphere with the inflation of the local evening sector greater than the inflation of the local morning sector. The recovery phase of the evening sector begins sooner and proceeds more rapidly than that of the morning sector so that the inflation becomes nearly symmetric during the final recovery to pre-storm levels.

PART 2: POLAR ELECTROJET

Geometry

Although the magnetic field of the earth is a vector field, the OGO-2 satellite measured only the (scalar) magnitude of this vector. We are therefore trying to deduce facts about a vector disturbance field from non-vector data. The magnitude of the main field at satellite altitude in polar regions is of the order of 40,000γ while the magnitude of the disturbance vectors are of the order of a few hundreds of gammas. If the disturbance vector is parallel to the main field vector of the earth, the change in magnitude of the field will be equal to the magnitude of the disturbance vector. If, however, the disturbance vector is orthogonal to the main field vector of the earth the main effect will be a change in direction with only a small change in magnitude. In this part we are mainly concerned with high latitude data ($> 60^{o}$N. Geographic Latitude) where the earth's field is almost vertical and, consequently, a vertical disturbance will be more readily detected at the satellite than will a horizontal disturbance.

Consider a single line current flowing at 105 km in the ionosphere (Figure 11, current is out of the figure) with an induced current oppositely directed 945 km below the earth's surface. The ratio 945/105 = 9 corresponds to a plane of infinite conductivity 420 km below the surface of a nonconducting earth. The ratio 9 was found by Scrase (1967) to best match his data at Lerwick and neighboring stations. Forbush and Casaverde (1961), while studying the equatorial electrojet in Peru,

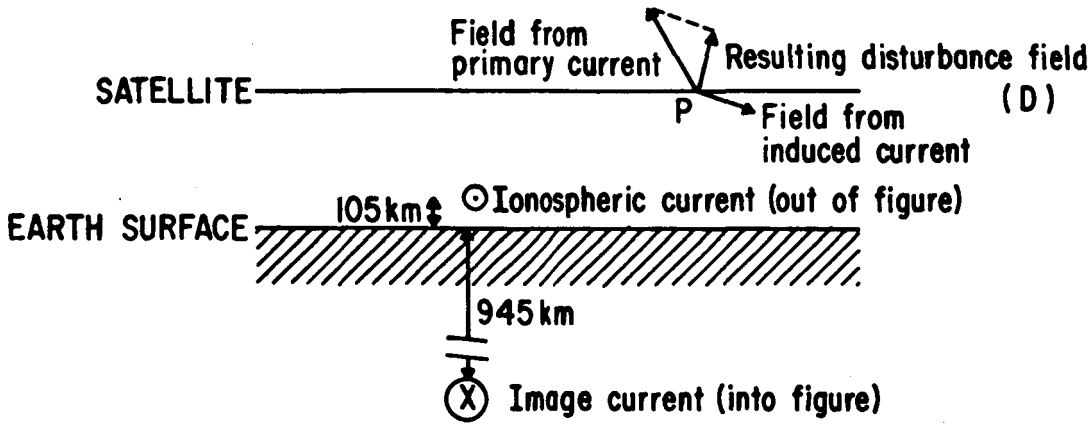

A. FIELD RESULTING FROM IONOSPHERIC LINE CURRENT AND IMAGE

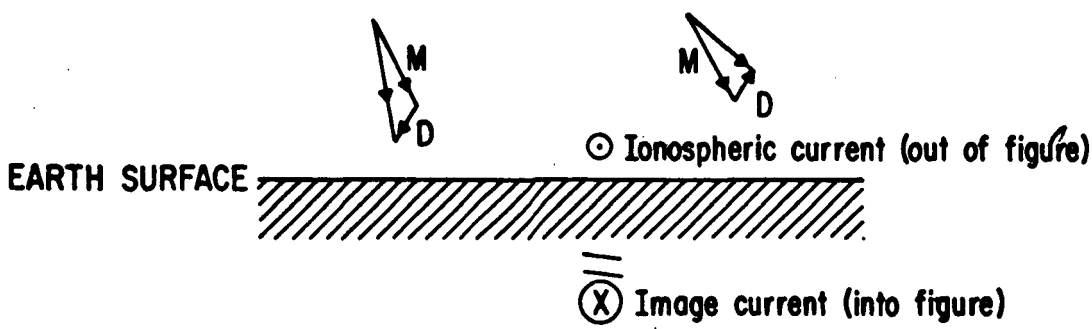

B. COMBINATION OF FIELDS FROM LINE CURRENT & EARTH'S MAIN FIELD.

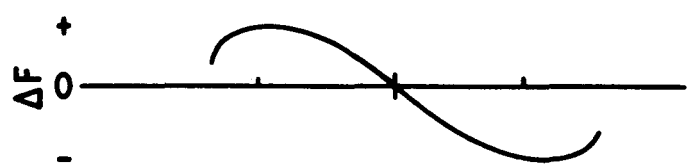

C. RESULTING ΔF AT SATELLITE: $\Delta F = |\bar{M}+\bar{D}| - |\bar{M}|$

SINGLE IONOSPHERIC LINE CURRENT AND RESULTING DISTURBANCE AT THE SATELLITE

FIGURE 11

used 150 km for the height of the ionospheric current and placed their image current at 650 km below the earth's surface. This gives a ratio of 4.33 between depth of induced current and height of ionospheric current. When experimenting with model current systems (see later this paper) we tried ratios between 1 and 9 and found 9 to give the best fit to the experimental data, although results did not differ greatly for ratio's between 4 and 9. Figure 11 illustrates the effect of an ionospheric current on the field as measured by the satellite. Part A of the figure illustrates qualitatively how the fields resulting from the ionospheric and induced currents add vectorially. If we take north to be to the right of the figure, then at point P, to the north of the currents, the field resulting from the currents will be mainly upward (i.e., negative Z) whereas to the south of the currents the resulting field would be mainly downward (positive Z).

Combination of the disturbance from the currents (D) with the main field of the earth (M) also takes place vectorially. Part B of Figure 11 illustrates this vector addition both north and south of the satellite and Part C indicates the general shape of the resulting ΔF at the satellite. ($\Delta F = | \vec{M} + \vec{D} | - | \vec{M} |$). The earth's main field (M) is mainly downward but also has a small northward component. North of the currents D will be mainly upward, resulting in a negative ΔF, and south of the currents D will be mainly downward resulting in a positive ΔF. If the ionospheric current of Figure 11 were oppositely directed, the peaks of the ΔF curve would be reversed. Thus it is

possible to deduce the general features of a current system from the ΔF curve measured by a satellite passing overhead. Of course, the same results at satellite altitude could be achieved by currents above the satellite. However, such a current would need to match variations observed at the surface.

The Satellite Data

Inspection of Figure 8 reveals the presence of a strong polar electrojet in both the northern and southern hemisphere. The largest indication is obtained at northern latitudes during the ascending portion of the orbit. A strong negative dip occurs, generally near 60° latitude, followed by a strong positive peak. As the satellite proceeds over the pole a weaker current is seen on the opposite side indicated by a negative dip followed by a positive peak as the satellite proceeds southward. The strong current in the (local) morning hours (ascending, 0500 local time) corresponds to a westward current while the weaker current in the evening (1530 hours local time) is mainly eastward with a weaker westward return current (to the north of the dip) also contributing substantially. Close examination of Figure 8 indicates that these currents are also present in the south polar region. The difference in the size of the effect from the currents in southern latitudes is explained by the fact that perigee is at about 72°N. latitude and apogee is in the south, with the result that the satellite is at altitudes below 500 km during its north polar transit but is above 1200 km during its south polar transit.

A Current Model

We have attempted to construct a crude model for the northern currents of the orbit shown in the middle of Figure 8 (beginning at 0329 UT, March 14th). The model consists of a series of infinite line currents spaced 1/2 degree apart in geographic latitude at an altitude of 105 km. Induced currents within the earth were assumed at a depth of 945 km; all currents are assumed to be parallel to the geographic equator. The series of infinite line currents is an approximation to a sheet current. This type of model was chosen because of its computational simplicity and because it is a reasonable first order approximation to the actual physical phenomena.

Figure 12 summarizes the derived current system and how the magnetic fields caused by the currents compare with the disturbance fields measured at both the satellite and the surface. The figure is in three parts with a common abscissa, geographic latitude. Part A (top) of the figure compares the disturbance field measured at the satellite (solid curve) with that resulting from the assumed current system (⊙ and ⊡). The ordinate is ΔF in gammas. Part B shows the assumed current distribution; the currents are located at the vertical tic marks. The ordinate indicates the current direction (+ for westward; - for eastward) and magnitude. Part C compares the disturbance field generated directly beneath the satellite (solid curve) with the disturbance measured at the surface very close to the satellite (within

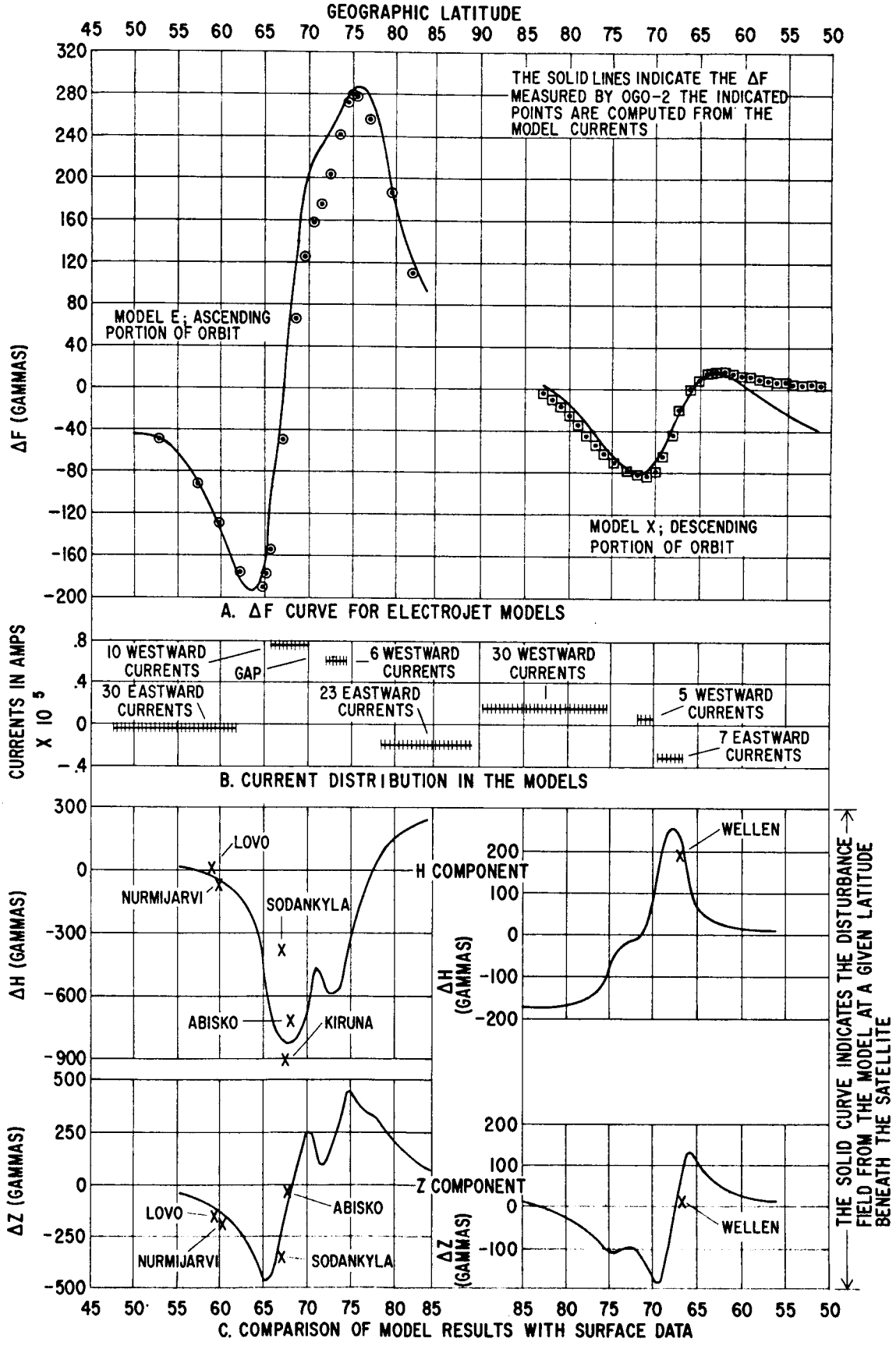

FIGURE 12: Disturbance fields from a polar current model compared with disturbances observed at OGO-2 and at surface observatories.

5° longitude). This comparison is done for both the horizontal (H) and vertical (Z) components with ordinates in gammas.

The agreement between the measured data and the disturbance computed from the assumed current distribution is good. The model matches the satellite data quite well in slope and in the locations and shapes of the dips and peaks. The most inaccurate match occurs near the inflection at 72.5° when the satellite is northbound and also below 60° when the satellite is southbound. In order to match the downward slope below 60° it would be necessary to include some eastward current in the latitude range 50-58°; however, the effects of the ring current may be enough at these latitudes to provide the 10-20γ difference between the model and the measured ΔF.

Zmuda et al. (1966) observed an average width of disturbance in the polar regions of about 6° on nightside (2300-0100 LT) passes and ≥ 8° on day side (1000-1400 LT) passes; Kp was ≥ 4 . This is in good agreement with the width of the currents as seen by OGO-2. Our model, for example, gives a morning (0500 LT) width (geographic) of 9.5° and an evening (1530 LT) width of 3°. The other currents seen by OGO-2 are of similar widths. The currents in our model (morning electrojet) go to zero (or a very low value) at ~ 72.5° to match an inflection in the data. This inflection is present in four out of the seven morning electrojets seen and we presently have no reason to doubt the existence of a gap in the currents at this latitude.

The total current is 1.1 million amperes in the westward jet and .224 million amperes in the eastward jet. This gives a total of 1.3 million amps. The total return current is about one million amps.

Considering that changes of 30% in the return currents would not affect the models appreciably, we would say that, to the accuracy of this model, all of the currents are accounted for.

The overall current distribution is given in Figure 13, in a (polar) coordinate system of geographic latitude (above 40°) versus local time, at approximately 0347 UT on March 14th. The approximate satellite path is shown and short lines perpendicular to this path indicate current intensity (~ 100,000 amperes flows between successive lines) and direction. The two "electrojets", westward at local time ~0500 and eastward at local time ~1530 are located at the maximum current density which is indicated by a maximum bunching of lines. For reference purposes the dip pole, location of 80° dip and the direction of Greenwich are indicated on the figure.

Current Locations

Previous discussions and models of polar currents (e.g. Akasofu, 1965; Vestine, 1949) have considered that they were organized in terms of a geomagnetic (dipole) coordinate system. We have examined the locations of the currents seen by OGO-2 in terms of not only dipole coordinates but also dip latitude and McIlwain's L parameter to determine which system provides the best reference. Table 1 is a list of all indications of the presence of major polar currents in the OGO-2 data during the course of the March 13-15 storm. The latitude given is the midpoint between dip and peak; L, dip latitude, and dipole latitude are derived directly from the geographical position. The table also includes the value (in gammas) of the range of

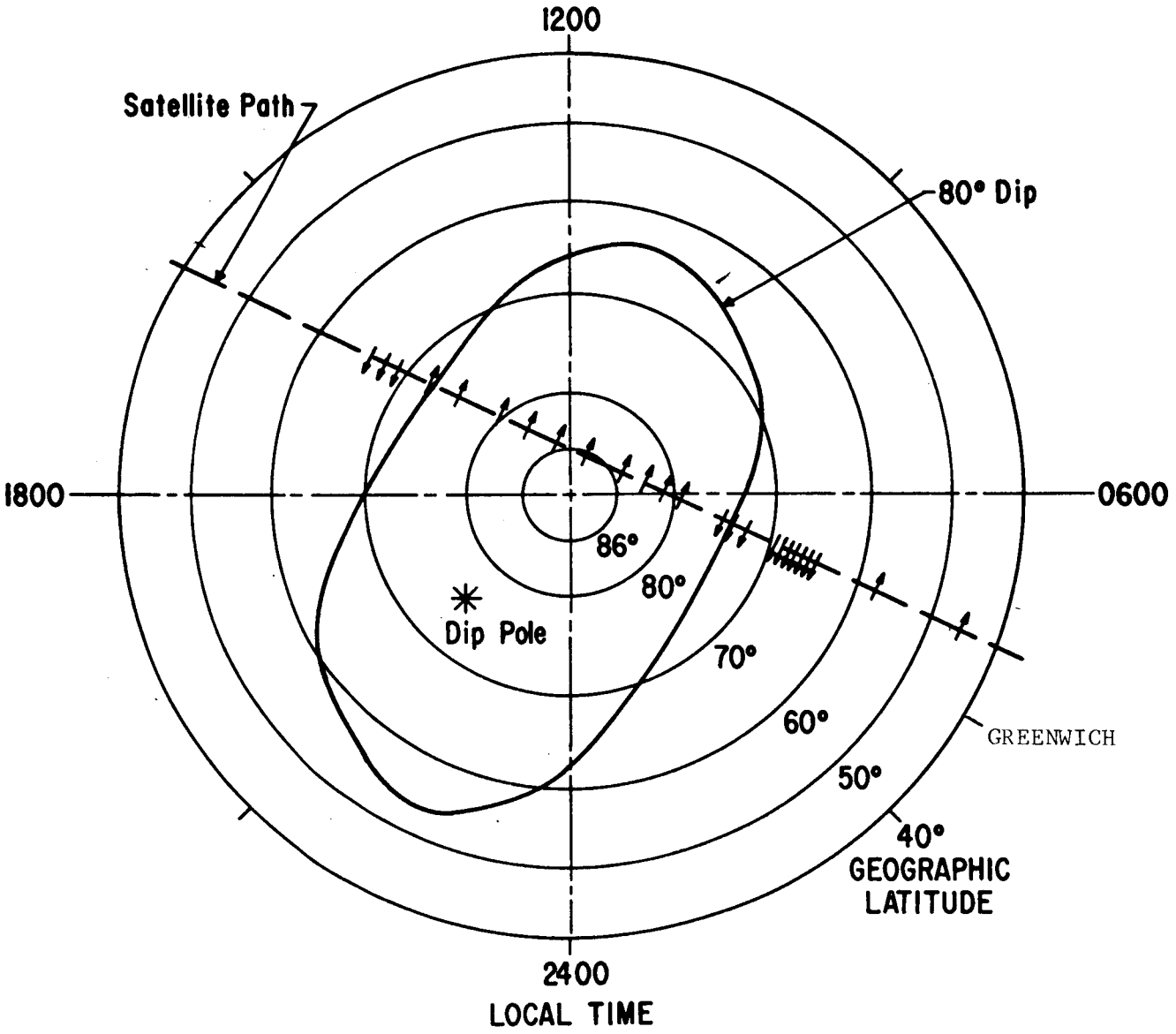

100,000 amperes flows between arrows.

POLAR IONOSPHERIC DISTURBANCE CURRENT DISTRIBUTION AS DETERMINED FROM OGO-2 DATA AT 0347 U.T. MARCH 14, 1967

FIGURE 13

Table 1 - High Latitude Currents

A. Morning (North Latitude, Ascending, 0500 local time)

Current Number	Date	U.T.	Latitude	Longitude	L	Peak-Peak Disturbance	Dip Latitude	Dipole Latitude
1	13th	1538	?	-159°	--	>150γ	--	--
2	13th	1725	74°	177	7.9	157	70	67
3	13th	2235	74.5	100	7.3	430	77	63
4	14th	0019	73.5	73	7.1	410	77	64
5	14th	0347	69.75	19	6.4	485	65	67
6	14th	1040	?	-87	--	--	--	--
7	14th	1220	56.0	-112	5.3	390	67	63

B. Evening (North Latitude, Descending, 1530 local time)

Current Number	Date	U.T.	Latitude	Longitude	L	Peak-Peak Disturbance	Dip Latitude	Dipole Latitude
8	13th	1542	71.25°	+9°	7.5	100γ	62	70
9	13th	1732	63.5	-15	5.5	69	61	68
10	13th	2250	52	-96	5.0	120	69	62
11	14th	0355	66.5	-174	4.6	100	61	61
12	14th	0905	69	107	4.9	190	73	58
13	14th	1055	66.25	81	4.3	190	68	56
14	14th	1240	68	55	4.9	230	67	60
15	14th	1425	66.25	28	4.8	135	61	63

disturbance at the satellite. Morning and evening currents are listed separately but otherwise the lists are ordered by time. In all discussion herein L is computed using only a main field model. Thus major distortions of the magnetosphere which undoubtedly occur during a disturbance could alter the L values obtained. However, this parameter can still be useful even though it may no longer be able to serve as an exact reference for trapped particles.

Variation of the current locations according to dip latitude is very irregular but the data do seem to organize well with respect to the dipole latitude and L parameter. Gradual commencement of the storm begins about 1900 hours UT on the 13th which is between current 2 and 3 in the morning and 9 and 10 in the evening (see Table 1). In both morning and evening, L and dipole latitude drop significantly before and during this time interval. For the morning current, the dipole latitude is then quite constant except for current No. 5 which is $\sim 4^{o}$ north of the surrounding currents. The evening currents continue to move southward in dipole latitude as the main phase of the storm proceeds and then move northward at about the same time as the rapid recovery from asymmetric inflation (See Part 1). The L value for the current locations behaves somewhat differently than the dipole latitude, decreasing steadily during the course of the storm for the morning currents but remaining quite constant in the evening. No particular change in L is noticed at the times that the magnetosphere is changing from asymmetric to symmetric inflation.

Discussion

Comparison of Figure 13 with Figure 1 shows a striking similarity between our model results and the two-celled model of polar disturbance currents. Thus, for this storm, the satellite evidence is that the two-celled configuration prevailed throughout.

In the one-celled polar electrojet model of Akasofu et al. (1965), the salient feature is an intense westward current encircling the dipole along what is called the auroral oval. This oval is discussed extensively by Akasofu (1966); it is defined as the instantaneous belt along which auroras tend to lie. Akasofu states that the orientation of the oval is fixed in local time and that the auroral zone ($\sim$ dip latitude 67^{o}) is the locus of the intersection of the midnight meridian with the oval. The oval latitudes are a function of storm activity (Dst), expanding southward as storm activity increases. According to Figure 1 of Akasofu's paper (1966), OGO-2 passes through the average location of the auroral oval between 66^{o}-73^{o}N. dipole latitude on the ascending (morning) portion of the orbit and between 76^{o}-78^{o}N. dipole latitude on the descending (evening) leg of the orbit. If the electrojet currents were strongly related to the oval, one would expect the observed currents to lie approximately within these ranges. Furthermore, one would expect the locations of the currents to "organize" well with respect to dipole latitude in that if the current locations changed significantly they would move to lower dipole latitudes with increasing Dst. Assuming that the oval moved southward from its average location during the storm, the initial downward motion in

dipole latitude between currents 1 and 3 would be the type of behavior expected from Akasofu's model. However, the highest dipole latitude (current 5) corresponds to the time of minimum Dst contrary to what one would expect. The evening electrojet, being eastward, does not fit this model at all.

In assessing the concept of the auroral oval, at least for this storm, one must conclude that, if the locations of the currents seen by OGO-2 are related to the oval location, the oval location would be described better in terms of McIlwain's L parameter than in terms of dipole latitude. Indeed, Zmuda et al. (1966 and 1967) describe the location of the oval using the parameter $\Lambda = \cos^{-1}[1/L]^{\frac{1}{2}}$ instead of dipole latitude. They discuss the location of a disturbance region, as determined by satellite data, relative to the oval and show that during geomagnetic quiet times ($Kp < 4$) the position of this disturbance region agrees well with the location of the auroral oval (using this Λ to describe the position of the oval) and that the location of the oval moves southward during more disturbed periods of time.

As Table 1 clearly shows, the position of the eastward electrojet at 1530 hours local time, and therefore the position of maximum disturbance at OGO-2 positions, is more southerly (in all coordinates, including L) than the westward electrojet at 0500 hours local time. This is different from the phenomena found by Zmuda et al. (1967) and, if (as described by Akasofu) the oval is at higher latitudes at 1530 than at 0500 local time, would place the largest current concentration at this local time, south of the auroral oval. In this case, the

currents in the auroral oval are, indeed, all westward as Akasofu et al. have suggested but the heaviest concentration of current in the evening local time section is eastward and is located to the south of the oval.

The first substantial currents seen by OGO-2 for this storm are 1, 2, 8, and 9 of Table 1. Similarly, currents 7 and 15 are the last to be detected and a satellite pass at 0045 on March 15 shows no evidence of major currents. Chapman (1956), and Davis and Sugiura (1966) have pointed out that polar current systems develop well before the main phase of magnetic storms. In support of this we note that currents 1, 2, 8, and 9 are more than 1.5 hours prior to the start of the gradual commencement of this storm. Sugiura (1967) has pointed out that there is a tendency for a_p to recover more rapidly than Dst after a magnetic storm and that this implies that the polar disturbances disappear more quickly than does the ring current. In Part 1 we showed that the ring current is asymmetric with more inflation in the evening local time sector, that recovery in the evening sector begins sooner than in the morning ($\sim$ 1200 UT on the 14th), and that the evening disturbance decays to a value nearly equal to the disturbance in the morning sector after which both sectors recover together. The disappearance of the polar electrojet as seen by OGO-2 takes place after 1430 UT on the 14th of March and before 0045 on March 15th, precisely the time period during which the evening ring current decays to the level of the morning ring current. This indicates some type of strong connection between the two phenomena, although the details remain unclear. (For example, Cummings, 1966, model of an asymmetric ring current with ionospheric return currents.)

ACKNOWLEDGMENTS

The instrumentation for this experiment was carried out under the direction of J. P. Heppner by W. H. Farthing and W. C. Folz of Goddard Space Flight Center. We also wish to thank L. McCarter and R. Hornstein for their aid in computer programming, Shirley Hendricks for performing some of the computation and for valuable discussion, and Dr. M. Sugiura for valuable discussion and suggestions.

The valuable contribution of the numerous magnetic observatories in quickly supplying copies of their records to the World Data Centers and the U. S. Coast and Geodetic Survey in supplying the surface data are also gratefully acknowledged. Observatory data used included:

Abisko	Honolulu	Sodankyla
Almeria	Kiruna	Stepanovka
Bangui	Lovo	Tananarive
Ebro	M'Bour	Tucson
Furstenfeldbruck	Nairobi	Vysokaya Dubrava
Guam	Nurmijarvi	Yangi-Bazar
Hartland	Pilar	Wellen
Hermanus	San Juan	

REFERENCE

Akasofu, S-I., The auroral oval, the auroral substorm, and their relations with the internal structure of the magnetosphere, Planetary Space Sci., 14, 1966.

Akasofu, S-I., and S. Chapman, On the asymmetric development of magnetic storm fields in low and middle latitudes, Planet. Space Sci., 12, pp. 607-626, 1964.

Akasofu, S-I., Chapman, S., and C-I. Meng, The polar electrojet, J. Atmospheric Terrest. Phys., 27, 1965.

Cahill, L. J., Inflation of the inner magnetosphere during a magnetic storm, J. Geophys. Res., 71, No. 19, October 1966.

Cain, J. C., I. R. Shapiro, J. D. Stolarik, and J. P. Heppner, Vanguard 3 magnetic field observations, J. Geophys. Res., 67, No. 13, December 1962.

Cain, J. C., S. J. Hendricks, R. A. Langel, and W. V. Hudson, A proposed model for the international geomagnetic reference field - 1965, NASA/GSFC Report X-612-67-173, July 1967.

Cain, J. C., R. A. Langel, and S. J. Hendricks, First magnetic field results from the OGO-2 satellite, Space Res., 6, 1967.

Chapman, S., Proc. Roy. Soc. London, A95, 61, 1919.

Chapman, S., Proc. Roy. Soc. London, A115, 2425, 1927.

Chapman, S., Terrest. Magnetism Atmospheric Elec., 40, 349, 1935.

Chapman, S., Ann. Geofis. Rome, 5, 481, 1952.

Chapman, S., The morphology of geomagnetic storms and bays: A general review, Vista in Astronomy, 2, 912-928, 1956.

Cummings, W. D., Asymmetric ring currents and the low-latitude disturbance daily variation, J. Geophys. Res., 71, No. 19, October 1966.

Davis, T. N., and M. Sugiura, Auroral electrojet activity index AE and its universal time variations, J. Geophys. Res., 71, No. 3, February 1966.

Farthing, W. H., and W. C. Folz, Rubidium vapor magnetometer for near earth orbiting spacecraft, Rev. Sci. Instr., 38, No. 8, 1023-1030, August 1967.

Furbush, S. E., and M. Casaverde, Equatorial electrojet in Peru, Carnegie Inst. of Wash. Pub. 620, 1961.

Hendricks, S. J., Personal communication, July 1967.

Heppner, J. P., J. D. Stolarik, and L. H. Meredith, Annals of the IGY, 6, 323, 1958.

Langel, R. A., Processing of the total field magnetometer data from the OGO-2 satellite, NASA/GSFC Report X-612-67-272, June 1967.

Parker, E. N., Non-symmetric inflation of a magnetic dipole, J. Geophys. Res., 71, No. 19, October 1966.

Scrase, F. J., The electric current associated with polar magnetic substorms, J. Atmospheric Terrest. Phys., 29, 1967.

Sugiura, M., and S. Chapman, The average morphology of geomagnetic storms with sudden commencement, Abl. Akad. Wiss. Göttingen, Math-Phys. Kl, Sonderheft Nr. 4, 1960.

Sugiura, M. Hourly values of equatorial Dst for the IGY, Annals of the IGY, 35, 1964.

Sugiura, M., and S. Hendricks, Provisional values of equatorial Dst for 1961, 1962, and 1963, NASA Technical Note D-4047, August, 1967.

Vestine, E. H., Isabelle Lange, Lucile Laporte, and W. E. Scott, The geomagnetic field, its description and analysis, Carnegie Inst. of Wash. Pub. 580, 1949, reprinted 1959.

Zmuda, A. J., J. H. Martin, and F. T. Heuring, Transverse magnetic disturbances at 1100 kilometers in the auroral region, J. Geophys. Res., 71, No. 21, November 1966.

Zmuda, A. J., F. T. Heuring, and J. H. Martin, Dayside magnetic disturbances at 1100 kilometers in the auroral oval, J. Geophys. Res., 72, No. 3, February 1967.